

Uses of Co-ZIF/67 and Zn-ZIF/8 in cathode materials and separators for Lithium batteries.

A Thesis

submitted to

Indian Institute of Science Education and Research Pune in partial fulfilment of
the requirements for the BS-MS Dual Degree Programme

by

Vyshnav Mohan



Indian Institute of Science Education and Research Pune

Dr. Homi Bhabha Road,

Pashan, Pune 411008, INDIA.

April, 2020

Supervisor: Dr.B.B.Kale , CMET, Pune

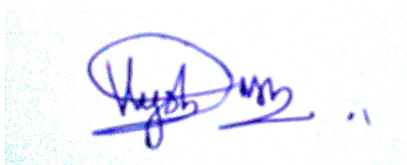
Vyshnav Mohan

All rights reserved .

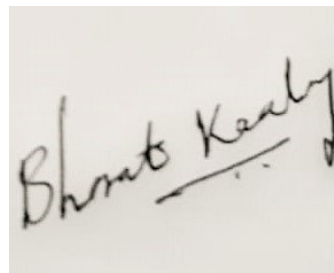
**Uses of Cobalt based ZIF/67
and Zinc based ZIF/8 in
cathode materials and
separators for Lithium
batteries.**

Certificate

This is to certify that the dissertation entitled ,”**Uses of Cobalt based ZIF/67 and Zinc based ZIF/8 in cathode materials and separator for Lithium batteries**”submitted by **Mr. Vyshnav Mohan** (20151187) as a project work requirement towards partial fulfilment of the BS-MS dual degree programme at the **Indian Institute of Science Education and Research, Pune** which was carried out during the period of **May 2019 - March 2020** at the **Centre For Material For Electronics Technology** under the supervision of **Dr B.B.Kale** ,Director , CMET Pune.



VYSHNAV MOHAN
BS-MS student
(Reg. No. 20151187)



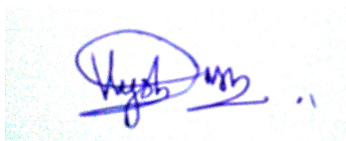
Dr. B.B.KALE
(SCIENTIST -G)
CMET, PUNE

Date:

Place: Pune, India

Declaration

I hereby declare that the project entitled “**Uses of Cobalt based ZIF/67 and Zinc based ZIF/8 in cathode materials and separator for Lithium batteries**” are the result of work carried out by me at the **Department of Polymer Chemistry** under the guidance of **Dr.B.B.Kale, CMET, Pune**. I further declare that it is my genuine work and has not been done previously for the award of any degree. The empirical findings in this report are based on data collected by me during the course of the project work.



VYSHNAV MOHAN

Acknowledgement

This master's thesis was carried out at the Department of Chemistry, Centre For Material For Electronics Technology, Pune between May 2019 and March 2020. This study was done as a part of the BS-MS programme conducted by IISER Pune. I would like to appreciate the following people for their help support and positive criticism during this study. Firstly I would like to thank my supervisor and mentor, Dr B.B.Kale, for giving me an opportunity to be involved in this study. I especially wanted to thank his support and guidance during the entire study.

Special Regards and appreciation to my co-supervisors Dr.Nageshwar Khupse and Dr. Trupti Nirmale for sharing their knowledge and experience which was really useful for completing this study. I would also like to show my gratitude towards Dr.J.D Ambedkar ,Dr.Marimuttu,Dr.Arul Kashir and Mr Sabeh More, for their ever-present helping hand, making the experiences resourceful and educating. My regards also goes to Arya Ajeev, Ashik V, Anjali and Sayali for their time and dedication towards my studies.

Lastly and importantly, I would like to sincerely thank my Acha, Amma and my Brother, Rahul for their help and love during the hard times.

ABSTRACT

The need of the generation is an energy source which is capable of quick charging, which cannot compromise on durability as well as high specific capacity^[1,2]. The Lithium Sulfur based batteries can satisfy all these needs which has a theoretical capacity of 1680 mAh g⁻¹ and surprisingly this is five times of the conventional batteries used currently^[3]. The abundance of sulfur, non-toxicity in nature, really large specific capacity as well as gravimetric capacity (2600 Watt hour per kilogram) show the huge potential of LSBs in the coming generations.

The commercial application of LSBs faces several issues. Sulfur is an insulator and thus facing poor kinetics in the electrochemical applications and highly resisting the free movements of electrons.^[4] Another serious issue is the production of polysulfides which causes active cathode mass loss as well as pulverization in the electrochemical cell.^[5] To overcome these issues; it is an accepted strategy to incorporate sulfur with composites whose conductivity is higher and shows much more longer cyclability.

Metal-organic framework (MOF) acts as a sulfur host, effectively trapping polysulfides and also increasing the electric conductivity. ZIF-67 and ZIF-8 have proved to effectively bind sulfur to its pores^[6,7]. Morphological studies were carried out for the MOFs using techniques like XRD, SEM, and FESEM. The use of these MOFs as separators were also studied at the later stages of the project. The electrospinning technique was used to obtain the nanofibers, which have the potential to replace the commercial Celgard due to a much better porous structure.

Contents

1. Introduction

- 1.1 Background and motivation
- 1.2 Basic principles of LSBs
- 1.3 Challenge for LSBs
- 1.4 Potential Solutions
- 1.5 Discussion on mofs in LSBs
- 1.6 Electrospinning Technique

2. Experimental Section

- 2.1 Chemical and materials
- 2.2 Synthesis
 - 2.2.1 Preparation of Co based ZIF/67
 - 2.2.2 Preparation of Zn based ZIF/8
 - 2.2.3 Preparation of ZIF/(67or 8)-Carbon-nanotubes
 - 2.2.4 Preparation of ZIF-67-Carbon-nanotubes/Sulfur
 - 2.2.5 Preparation ZIF-8 -Carbon-nanotubes/Sulfur
 - 2.2.6 Electrode preparation
 - 2.2.7 Preparation of MOF(ZIF8/ZIF67)-PVP solution
- 2.3 Cell setup
 - 2.3.1 LSBs setup
 - 2.3.2 LSBs@ZIF67/ZIF8-CNTs/S setup
 - 2.3.3 Li-ion Setup with MOF separators
- 2.4 Instruments used
 - 2.4.1 Powder X-ray diffraction

2.4.2 Scanning electron microscope

2.4.3 Field Emission Transmission electron microscope

2.4.4 Electrospinning Machine

3. Results and discussion

3.1 Characterization of Synthesised Materials

3.1.1 X-ray diffraction

3.1.2 Scanning electron microscope

3.2 Flaws in the Slurry preparation

3.2.1 Images of Comparison of Different slurry composition for LSBs.

3.2.2 Discussion on why it might have happened.

3.3 Electrospinning analysis

3.3.1 Scanning electron microscope.

3.3.2 TEM images

3.3.3 Images of the fibers obtained.

3.3.4 Discussion on how the fibres will be used.

4. Conclusion

5. Future outlook

6. Reference

List of figures

Label	Description	Page no
Fig 1.1	(a) Formation of polysulfides during the charge/discharge potential profile (b)The working of a Lithium-Sulfur battery with charge/discharge processes	12
Fig 2.1	The synthesis scheme of ZIF/67 TO ZIF/67-carbon-nanotubes/sulfur	18
Fig 2.2	Powder X-ray diffractometer	21
Fig 2.3	Schematic diagram of Scanning electron microscope	22
Fig 2.4	ESPIN NANO electrospinning machine	23
Fig 3.1	pXRD (a) Sulfur (b) ZIF67-Carbon-nanotubes ,(c,d,e) ZIF/67-carbon-nanotubes/Sulfur	25
Fig 3.2	pXRD (a) Sulfur (b)ZIF/8 (c)ZIF/8-Carbon-nanotubes(d) ZIF/8-carbon-nanotubes/Sulfur	26
Fig 3.3	Electron microscope images of ZIF/8	27
Fig 3.4	Electron Microscope images of ZIF/67	27
Fig 3.5	(a)Electron microscope images of ZIF/67-Carbon-nanotubes showing	28

	pores.(b)Electron microscope images of ZIF/8-Carbon-nanotubes.	
Fig 3.6	Non homogeneous slurry after coating on the sheets.	29
Fig 3.7	(a) Electron microscope images of ZIF/8 in polyvinylpyrrolidone at lower resolution (b) Electron microscope images of ZIF/8 in polyvinylpyrrolidone at higher resolution	30
Fig 3.8	(a) TEM images of ZIF/8 in polyvinylpyrrolidone at lower resolution (b) TEM images of ZIF/8 in polyvinylpyrrolidone at higher resolution	31
Fig 3.9	(a) ZIF/8 in polyvinylpyrrolidone (b) ZIF/67 in polyvinylpyrrolidone	32

List of Abbreviations

CC	Conducting Carbon
CNTs	Carbon Nanotubes
CV	Cyclic Voltammetry
FESEM	Field Emission Transmission Electron Microscope
DME	1,2-Dimethoxyethane
DOL	1,3-,Dioxlane
LiTFSi	Lithium bis(trifluoromethanesulfonyl)imide
LSBs	Lithium Sulfur Batteries
MOF	Metal Organic Framework
OCV	Open Circuit Voltage
PVDF	Poly Vinylidene Fluoride
PVP	Poly VinylPyrrolidone
SEM	Scanning Electron Microscope
pXRD	Powder XRay Diffraction
ZIF/8	Zinc based Zeolitic Imidazole Framework
ZIF/67	Cobalt based Zeolitic Imidazole Framework

1. INTRODUCTION

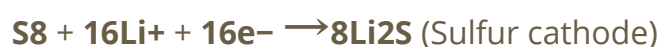
1.1 Background and motivation

The commercialization of Lithium-ion batteries (LiBs) in the 1990s. After the introduction of LiBs, the market has been dominated by this lithium based electrochemistry for over more than 25 years. This was then due to their energy density of around 160-260 Wh Kg⁻¹, large potential, and relatively large cycling stability^[8]. But in recent years, we are approaching the theoretical limits of energy density for these LiBs, and these are insufficient for satisfying our growing energy requirements. Thus the need for new electrochemistry and cathode materials is necessary.

Lithium-Sulfur Batteries (LSBs) are one of the strong contenders to provide the world with sufficient energy in the coming years. The advantages of using LSBs include high theoretical capacity which is around 1680 mAhg⁻¹ and gravimetric density around 2600 Watt hour per kilogram.^[6,8] This energy density is the combined use of sulfur-made cathode (1680 mAhg⁻¹) and lithiated anode (3860 mAhg⁻¹)^[9]. Sulfur has a high abundance in nature as it is a byproduct of the petroleum industry, and it is relatively cheap compared to the expensive transition metals like Lithium cobalt oxide and Lithium ferrous phosphate used in Lithium-ion batteries. The availability of these transition metals are also limited. They are also toxic in nature, whereas LSBs fit the bill for being environmentally-friendly too. These appealing advantages have led scientists across the globe to do research on LSBs.

1.2 Basic principles of LSBs

A basic Lithium sulfur battery (LSBs) contains a Lithiated anode and a sulfur cathode with electrolyte and a membrane (separator) between them. During discharge sulfur reacts with lithium ions forming lithium sulfides with different proportions and structure.^[10,11]



The discharge peaks of this voltage profile could be identified at 2.3 V and 2.1 V, this indicates the change from solid sulfur (S₈) to the high order liquid phase polysulfides (Li₂S_n) (which is the 2.3V) and then back to the lower order solid phase polysulfides (Li₂S₂/Li₂S) (2.1V).^[12,13]



Both of the overlapping anodic plateaus are identified exactly at 2.4 V and 2.5 V. This indicates that the polysulfides are rapidly converting back to sulfur.

During these processes, the produced polysulfides dissolves in the electrolyte which then leads to loss of effective mass of the electrodes. Thus attaining the theoretical capacity of 1680 mAh g⁻¹ is challenging enough for the LSBs^[14,15]

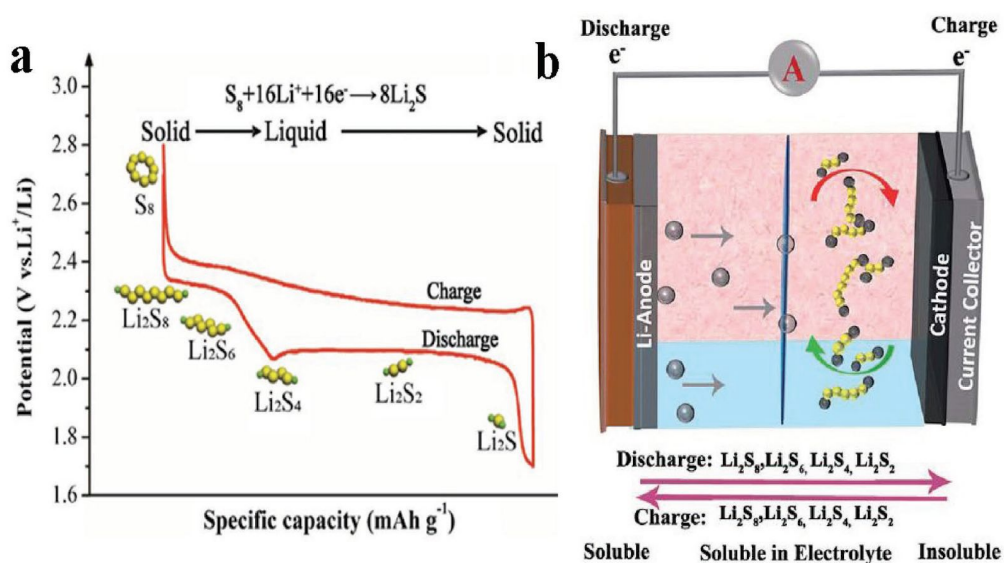


Fig 1.1 (a) Formation of polysulfides during the charge/discharge potential profile. Copyright 2017, Wiley-VCH^[10] (b) The working of a Lithium-Sulfur battery with charge/discharge processes, the Royal society of chemistry. ^[16]

1.3 Challenges of LSBs

Commercial applications of LSBs are limited by several barriers. First and foremost is that sulfur is a bad conductor of electricity. Sulfur and LiS are insulators having electrical conductivities of 5×10^{-30} S cm⁻¹ and 10-13 S cm⁻¹ respectively^[17]. The insulating Li₂S can precipitate on the conducting materials, which can cause a decrease in the voltage during the last step of the discharge process. Because of the bad kinetics and high resistance in the electron movement (donor -acceptor mechanism) of active materials, large polarisation is favored to achieve the high theoretical capacity of LSBs.

During the charging and discharge process, polysulfides are formed. This includes Intermediates such as Li₂S_n, where n=2,4,6, which are soluble in ether-based electrolytes (commonly used for LSBs). The Dissolution of polysulfides not only produces loss of weight in the cathode (some voids) but also makes the electrolyte viscous, thus reducing the conductivity. The polysulfides also shuttle back and forth to the negative electrode and then precipitate into lower order polysulfides which are insulating and also highly insoluble. This is termed as “shuttling effect”, which results in the loss of sulfur, leading to higher resistance internally and also reducing the cycling capacity of the cell. The overall coulombic energy of the cell is also lost^[18,19]. Pulverization of the cell also occurs due to the repositioning of polysulfides onto the electrode. Thus leading to the short circuit. This is mainly due to the difference in densities of sulfur and Li₂S causing volume expansion. Due to this outcome, continuous expansion and contraction during the cycles. Thus questioning the safety measures and fast decay of capacity.^[10]

1.4 Potential Solution

Various methodologies are used to improve the performance of LSBs. This includes standardization of electrolytes, the proper trapping of sulfur and successfully holding not letting the lithium polysulfides to dissolve with physical parameters and chemical parameters. Recent works in the scientific world have shown progress in sulfur/carbon cathodes^[20,21,22] with different types of carbon nanotube composites being developed. Good fabrication and vast

diversities of this nanomaterials are required for achieving the high performance LSBs.

Trying to avoid electrolytes which can dissolve the polysulfides formed is also an important step in the betterment of the LSBs. In the case of electrolytes which are carbonate based, for example LiPF₆ in EC + DMC, the lithium polysulfides produced reacts with the carbonates irreversibly leading to the loss of electrode materials.^[23 to 26] But when ether based electrolyte were used instead of carbonate based ones, which is commonly LiTFSi in DOL/DME, the sulfur electrodes were operative. Thus using ether based electrolytes in this report for LSBs.

Shuttling effect is another disadvantage of LSBs causing inhomogeneous distribution of sulfur particles. The research on various carbon and carbon based composite to effectively incorporate sulfur and polysulfides in cathodes is regarded to be the most challenging as well as important. Carbon composites with different morphologies (including shape, size), porous structure and specific substituents has undergone research to incorporate sulfur also to trap lithium polysulfides in electrodes by physical parameter such as polarity and adsorption^[27, 28]. With their highly porous structures, the high surface area they provide as well as their morphologies which are controllable, MOFs are the perfect solution to this shortcomings.

1.5 Discussion on mofs in LSBs

Metal-organic framework (MOF) acts as a sulphur host effectively trapping polysulfides and increasing the electrical conductivity. The MOFs have specific functional groups which hold on to this sulfur and polysulfides through various interactions. One of the main advantages of metal organic framework is their morphologies which can be altered based on our need. MOFs have various sites in them which trap the incoming polysulfides and also not letting them dissolve in the electrolyte. This is achieved through polar-polar interactions. With their highly porous structures, the high surface area they provide as well as their morphologies which are controllable, MOFs are the perfect solution to the shortcomings of LSBs ^[29,30,31]

Zeolitic Imidazole framework, ZIFs have been used for this study. Both Cobalt based and Zinc based ZIFs have been synthesised and used. ZIF/8 and ZIF/67 are two noticeable MOFs capable of trapping Sulfur due their pore size comparable to that of a sulfur atom. ZIF-67 also shows a good performance in electrochemistry ^[32]. These two MOFs are really good as a sulphur host as their pore size is comparable to the size of the sulfur atom thus effectively trap sulfur species in cathodes. They are also easy to synthesis and it is environmental friendly which adds to the advantages against using toxic materials in lithium ion batteries.

1.6 Electrospinning technique

Electrospinning is a top down technique to help generate nanofibres from different polymeric solutions. This technique uses high voltage (in kV) to evaporate the solvent used and produce threads of polymer. The preparation of this nanofiber with high porosity, large surface area has been a challenge and MOFs are well known for their highly porous morphology and effective surface region ^[33]. ZIFs are also known for their unique chemical and heat tolerance. In this study was done to incorporate both ZIF/67 and ZIF/8 with the polymer to form nanofibers which can then be used as separators replacing the conventional celgard for better performance in any Lithium based batteries.

2. EXPERIMENT

2.1 Chemicals Used

Sr no	Chemical	Manufacturer	Purity
1.	Cobalt nitrate hexa-hydrate	Qualigens	98%
2.	Zinc nitrate hexa-hydrate	Fischer Scientific	98%
3.	2 methyl imidazole	TCI	98%
4.	Methanol (HPLC)	Chemi Labs	98%
5.	1,3 Dioxolane	TCI	98%
6.	1,2 Dimethoxyethane	TCI	99%
7.	Sulfur powder	Sigma aldrich	99%
8.	Lithium bis(trifluoromethanesulfonyl)imide	Sigma aldrich	99%
9.	Lithium Nitrate anhydrous	Fischer Scientific	98%
10.	Poly vinyl pyrrolidone	Alfa Aesar	--
11.	Celgard 2400	Celgard INC	--

2.2 Synthesis

2.2.1 Preparation of Co based ZIF/67

This procedure was previously reported in a research article^[34]. Firstly a solution containing 1 mole (around 3.07 grams) of Cobalt Nitrate hexahydrate dissolved in 25 mL methanol was prepared. Followed by dissolving 8 mol (around 6.93 grams) of 2-methylimidazole in 30 mL methanol. This two solution was stirred well under room temperature to form a homogenous solution. This solution was then left for precipitation around 24 hours. This was also done in room temperature. A deep purple ppt was found to be formed. This was then centrifuged at 4000 rpm, rinsed with methanol a few times to remove the excess 2-methylimidazole and finally dried at 80 degree for 12 hrs. It has been noticed that 1:8 ratio of $\text{Co}(\text{NO}_3)_2 \cdot 6\text{H}_2\text{O}$: 2-methylimidazole gives the highest yield and preferable pore size.^[35]

2.2.2 Preparation of Zn based ZIF/8

This procedure followed is similar to the one explained above. A solution containing 1 moles of $\text{Zn}(\text{NO}_3)_2 \cdot 6\text{H}_2\text{O}$ (around 6.2 grams) dissolved in 25 mL methanol. Followed by dissolving 8 moles of 2-methylimidazole (around 13.66 grams) in 30 mL methanol. This two solution was stirred well under room temperature to form a homogenous solution. This solution was then left for precipitation around 24 hours. This was also done in room temperature. A white ppt was found to be formed. This was then centrifuged at 4000 rpm, rinsed with methanol a few times to remove the excess 2-methylimidazole and finally dried at 80 degree for 12 hrs. It has been noticed that 1:8 ratio of $\text{Zn}(\text{NO}_3)_2 \cdot 6\text{H}_2\text{O}$: 2-methylimidazole gives the highest yield and preferable pore size.

Both the above solutions can be prepared by replacing methanol with deionized water also. But the particle size may vary and might not serve the purpose of this study.

2.2.3 Preparation of ZIF/67-Carbon-nanotubes and ZIF/8-Carbon-nanotubes

The ZIF-67 was firstly subjected to a nitrogen atmosphere at 300 degrees for 2 hours with a constant heating rate around 1.5 degree per minute, and then pyrolysed again in the nitrogen atmosphere at 600 °C for 6 hours with a

constant rate of 1 degree per minute. It is then cooled down to room temperature. Thus obtaining ZIF/67-Carbon-nanotubes.

Similarly ZIF-8 was also subjected to a nitrogen atmosphere at 300 degrees for 2 hours with a constant heating rate around 1.5 degree per minute, and then pyrolysed again in the nitrogen atmosphere at 600 °C for 6 hours with a constant rate of 1 degree per minute. It is then cooled down to room temperature. Thus obtaining ZIF/67-Carbon-nanotubes.

2.2.4 Preparation of ZIF/67-Carbon-nanotubes/Sulfur

The process of melt-impregnation method was used.^[36] The ZIF/67-Carbon-nanotubes was added with sulfur powder in the ratio 2:8. This was mixed thoroughly. Subsequently, the composite was prepared using the hydrotherm technique at 140 °C for 20 hours to associate sulfur into the porous structures of ZIF/67-Carbon-nanotubes. After cooling down to room temperature, ZIF/67-carbon-nanotubes/Sulfur was made.

2.2.5 Preparation of ZIF/8-Carbon-nanotubes/Sulfur

The process of melt-impregnation method was used. The ZIF/8-Carbon-nanotubes was added with sulfur powder in the ratio 2:8. This was mixed thoroughly. Subsequently, the composite was prepared using the hydrotherm technique at 140 °C for 20 hours to associate sulfur into the porous structures of ZIF/8-Carbon-nanotubes. After cooling down to room temperature, ZIF/8-carbon-nanotubes/Sulfur was made.

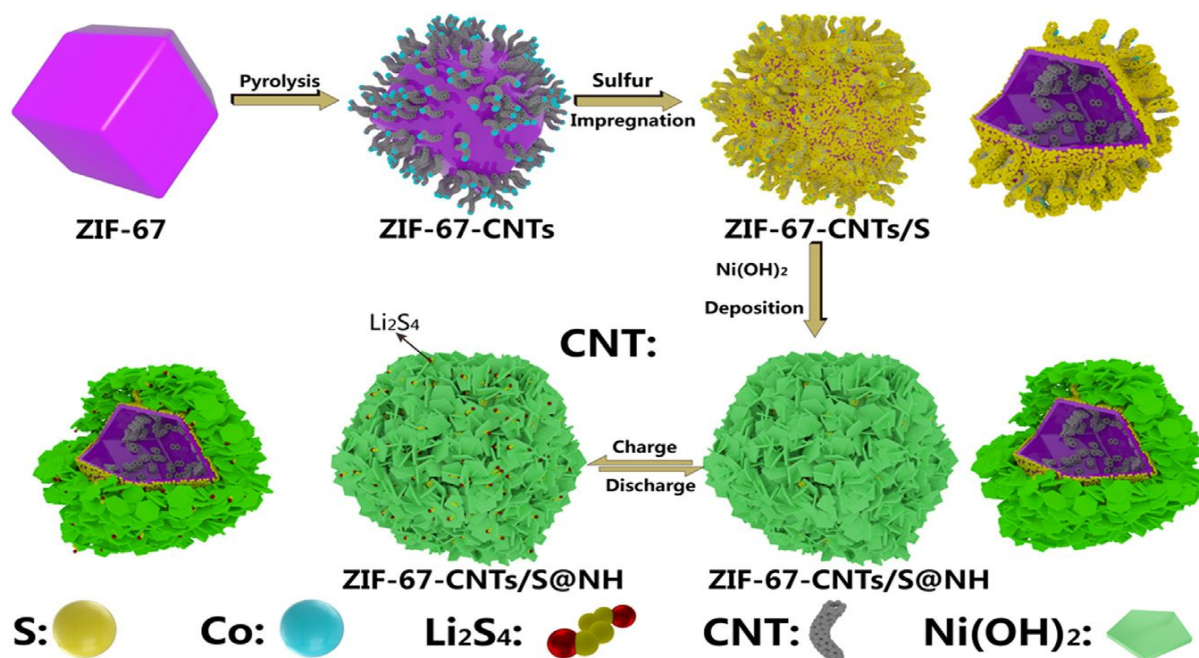


Fig.2.1. The synthesis scheme of ZIF/67 TO ZIF/67-carbon-nanotubes/sulfur (The last process was not carried out)from H.Wu et al.(2019) ^[34]

2.2.6 Preparation of Electrodes

For LSBs, the cathode was made by making a slurry with different proportions of substrate ,binders and solvents as the slurry prepared was not getting uniformly coated or being homogenous on the aluminum sheet.This was the challenge faced during this study.

For LSBs with sulfur as active material,the slurry was made with 50% conducting carbon (CC) by weight , 40% sulfur and 10% pvdf in N-Methyl-2-pyrrolidone, all of this adding up to a total weight of 200mg.This was then scaled up to 2g and 5g with the same proportions and substrate as the earlier to attain better results.For LSBs with active material as ZIF/67-Carbon-nanotubes/Sulfur or ZIF/8-Carbon-nanotubes/Sulfur ,the slurry was made with 80% active material,10% CC and 10% pvdf in N-Methyl - 2-pyrrolidone.This procedure was reported in H.Wu et al (2019).The prepared slurry was coated and then heated for 12 hours at 70 degrees in vacuum.Aluminum sheets were used.

2.2.7 Synthesis of MOF(ZIF8/ZIF67)-PVP solution

The solution of ZIF/8 and ZIF/67 were prepared as mentioned above.After the ZIFs are obtained after centrifugation it is re-dispersed in fresh methanol and sonicated.Around 3.5 - 4.5 wt% (around 0.350g) of this synthesised ZIFs was mixed in 5 mL of methanol.Another solution of 12 wt% pvp (molecular weight 1300000) around 0.6g in 5 mL was prepared and stirred for an hour.This two solution was mixed thoroughly and stirred for another hour under room temperature.A white homogenous solution is formed when ZIF/8 was used and deep purple solution in case of ZIF/67.Both of this homogeneous solution was effectively used for electrospinning.

2.3 Cell setup

2.3.1 LSBs setup

This coin cell was made by using sulfur cathode as prepared above, lithium anode and celgard 2400 (commonly used commercial separator). The preparation of the electrolyte was done by dissolving 1 mol of LiTFSI in 1:1 (v/v) in ether based solvents mainly, DOL and DME. 0.1 mol of lithium nitrate anhydrous was then mixed to complete the electrolyte.

2.3.2 LSBs@ZIF67/ZIF8-CNTs/S setup

This coin cell was made by using cathode which was prepared by making a slurry from mixing 75 % of ZIF composites (*ZIF8-Carbon-nanotubes/Sulfur* or *ZIF67-Carbon-nanotubes/Sulfur*), 15 % of CC, and 10 % polyvinylidene fluoride in N-methyl pyrrolidone (NMP) as reported in H.Wu et al. PvdF acts as a binder. Lithium was used as anode along with celgard 2400 membrane (commonly used commercial separator). The electrolyte was made by dissolving 1 mol of LiTFSI in 1:1 (v/v) in ether based solvents mainly, DOL and DME. 0.1 mol of lithium nitrate anhydrous was then mixed to complete the electrolyte.

2.3.3 Li-ion Setup with MOF separators

This is a conventional coin cell with lithium cobalt oxide as cathode, graphite based alloy as anode and commonly used lithium hexafluorophosphate in organic solution as electrolyte. The separator was a mixture of PVP and ZIF/8 or ZIF/67 which was prepared using the electrospinning technique. This was used as separator instead of the conventional celgard 2400 membrane. These membranes have porous polymeric nanofiber with high surface area due to the MOFs incorporated into the polymer fibres.

2.4 Instruments used

2.4.1 Powder X-ray diffraction

pXRD is an instrument which characterizes powdered crystals. Powder X-ray Diffraction (PXRD) uses the technique of diffraction principle to characterize crystalline nature of powder/material. The scattering of X-rays gives the atomic configuration in the crystalline material from the diffraction pattern produced by the respective atom. When X-ray falls upon a crystal, it produces diffraction peaks unique to the crystal. A diffraction pattern plots intensity versus the angle of the detector, 2θ . The X-ray diffracted satisfy Bragg's law if it is constructively interfered. This law gives the relationship between wavelength of the incident ray, incident angle of the beam and the spacing between the crystal lattice. Constructive interference happens when the path difference of the incident rays is equivalent to an integral product of its wavelength.

According to Bragg's law,

$$2d\sin\theta = n\lambda$$

where d is the distance between the Bragg planes, θ is the angle of incidence, λ gives the wavelength and n is an integer. The pXRD was done on D8 advance bruker diffractometer in iiser pune. The range of 2θ was from 5° - 85° .



Fig.2.2 Powder X-ray diffractometer(Physics at iiser pune image)

2.4.2 Scanning electron microscope

It is an electron microscope which creates images after shooting a beam of electrons onto the surface of the material. It helps in understanding the surface topology and composition of the sample. Secondary electrons which are then released by respective atoms after collision with electron beam are observed by the secondary electron detector. A small amount of compound (few milligram) was dispersed in few millilitres of ethanol and kept under sonication for 15 minutes. 4 μ l of the dispersion was drop-casted onto a silicon wafer and allowed to dry. The silicon wafers were later examined under SEM.

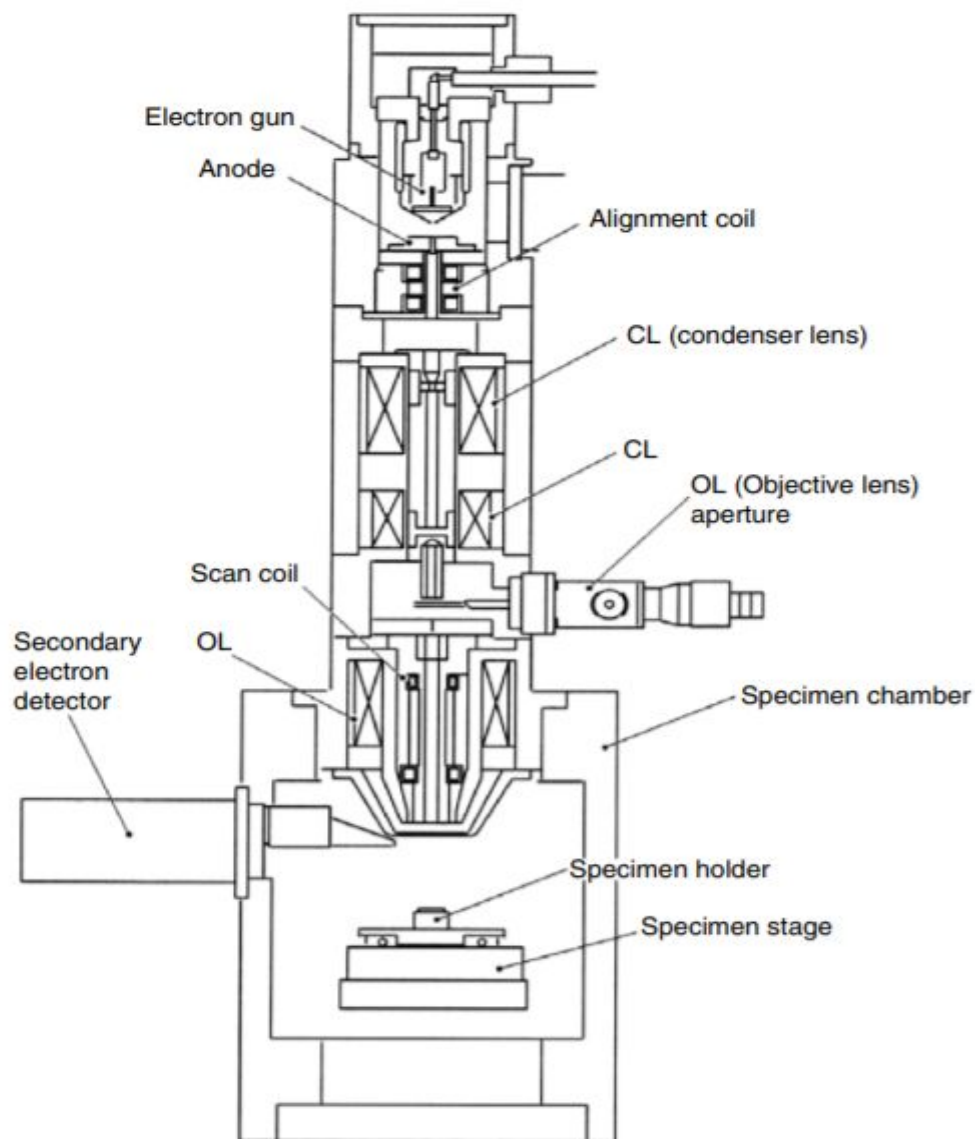


Fig.2.3 Schematic image of SEM (JSM-5410 ,courtesy of JEOL,USA)

2.4.3 Field Emission Transmission electron microscope

FETEM or TEM is similar to a SEM ,and the only difference in working principle is that it detects transmitted electrons instead of scattered electrons.Thus we can investigate the molecular surface structures and the electronic property of the sample materials.

2.4.4 Electrospinning Machine

Electrospinning technique is to help generate nanofibres from a wide variety of materials.This technique uses high voltage(in kV) to evaporate the solvent used and produce threads of polymer.Due to the high voltage the solution attains some charge,this electrostatic repulsion produced work against the surface tension and the droplets are sprayed as fibres after getting stretched.Due to the high voltage , constant elongation and thinning is produced.This elongation and thinning results in the uniform formation of fibres with diameter in the nanoscale region.

The needle was kept 6.5 cm away from the collector(standardized).The voltage needed was around 12 kilo volt,with a flowrate of 0.5 ml/hr and drum speed of 1013 rpm.This was run for a total of 10 mL homogeneous solution of polymer and MOF.

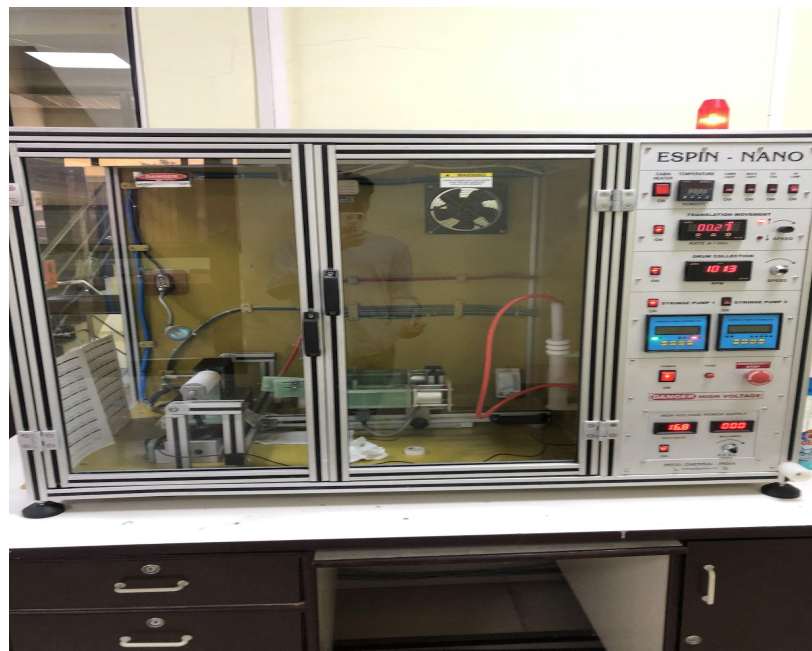


Fig.2.4 ESPIN NANO electrospinning machine in CMET pune

3.RESULT AND DISCUSSIONS

The results consist of two different types of experiments done over the course of this report. The first experiment was carried out for the majority duration until it was unable to proceed further and get any good results or observation within the limited time frame. The second experiment (electrospinning technique) was done over a short duration and had much success.

3.1 Characterization of Synthesized Materials

ZIF/67 dodecahedra and ZIF/8 dodecahedra were first synthesised as reported in the synthesis. The ZIF/67-Carbon-nanotubes was synthesized by pyrolysis of the deep purple ZIF-67 which consist of excess Carbon, Cobalt, and Nitrogen atoms in Nitrogen atmosphere. Similarly in the case of ZIF/8-Carbon-nanotubes which has excess Zinc instead of Cobalt. The ZIF-67-Carbon-nanotubes/Sulfur or ZIF/8-Carbon-nanotubes/Sulfur composite was obtained by introducing sulfur into the porous structure of the ZIF/67-Carbon-nanotubes and ZIF/67-Carbon-nanotubes using impregnation method. The morphology and microstructure was determined by SEM and TEM. The crystallinity of the synthesized compounds were determined using pXRD.

3.1.1 Powder X-Ray Diffraction

Comparing the pXRD data with the simulated sodalite structure ZIF/67 (JCPDS:30-0443), all the peaks are precisely indexed having reflections at $2\theta=7.4^\circ, 10.4^\circ, 12.7^\circ, 14.8^\circ, 16.5^\circ, 18.0^\circ, 22.1^\circ, 24.5^\circ, 25.5^\circ, 26.7^\circ, 29.5^\circ, 30.6^\circ, 31.6^\circ, 32.5^\circ$ corresponding to the (011), (002), (112), (022), (013), (222), (114), (233), (224), (134), (044), (334), (244) and (235). The ZIF/67-Carbon-nanotubes shows three peaks corresponding to the angles $31^\circ, 36.9^\circ, 44.9^\circ$ which can be then associated with the planes (2,2,0) (3,1,1) (4,0,0). (JCPDS no. 43-1003), respectively. After Sulfur is introduced to the composite already made, The peaks mainly arise due to the orthorhombic morphology of the sulfur. Thus showing the combination of the diffraction peaks of both ZIF/67-carbon-nanotubes and Sulfur for the composite ZIF/67-Carbon-nanotubes/Sulfur. But the intensity is slightly weaker in nature.

The pXRD analysis of the synthesized ZIF/8 shows peaks at around $2\theta = 7, 10, 15.80, 17.40$ and 19.00° correspond to the (1,1,0), (2,0,0), (2,1,1), (2,2,0), (3,1,0), and (2,2,2). We can observe peaks of ZIF/8-Carbon-nanotubes also formed but the peaks couldnt be clearly distinguished. It can be noticed that there is a clear decrease in the number of peaks after doping with Carbon-nanotubes ,which could be due to the presence of lesser amount of MOF. It can be due to the high dispersion of Carbon-nanotubes in ZIF-8. This indicates the proper dispersion of carbon-nanotubes in MOF . ZIF/8-Carbon-nanotubes/Sulfur showed even less precise pXRD and no reported data was available to compare.

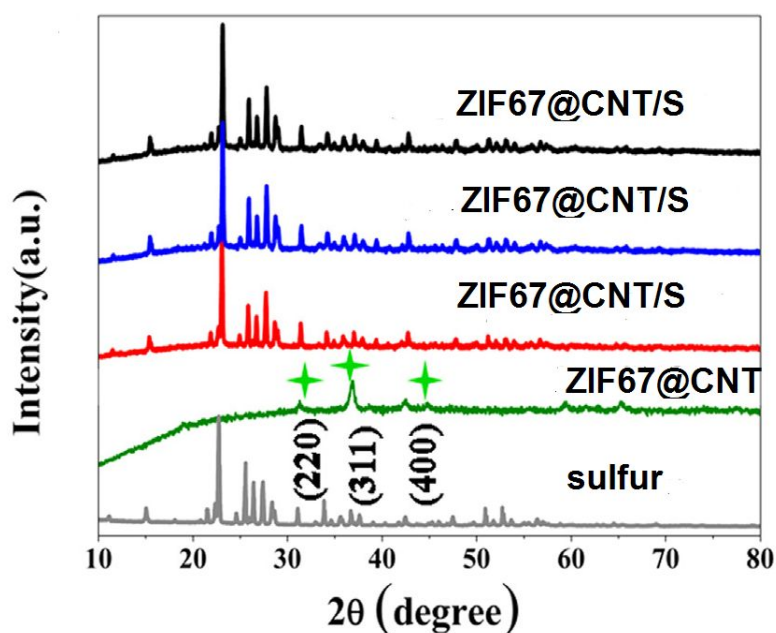


Fig.3.1 pXRD images of (a) Sulfur (b) ZIF/67-Carbon-nanotubes,(c) (d) and (e) ZIF/67-Carbon-nanotubes/Sulfur prepared at different stages of the report with most of the patterns matching.

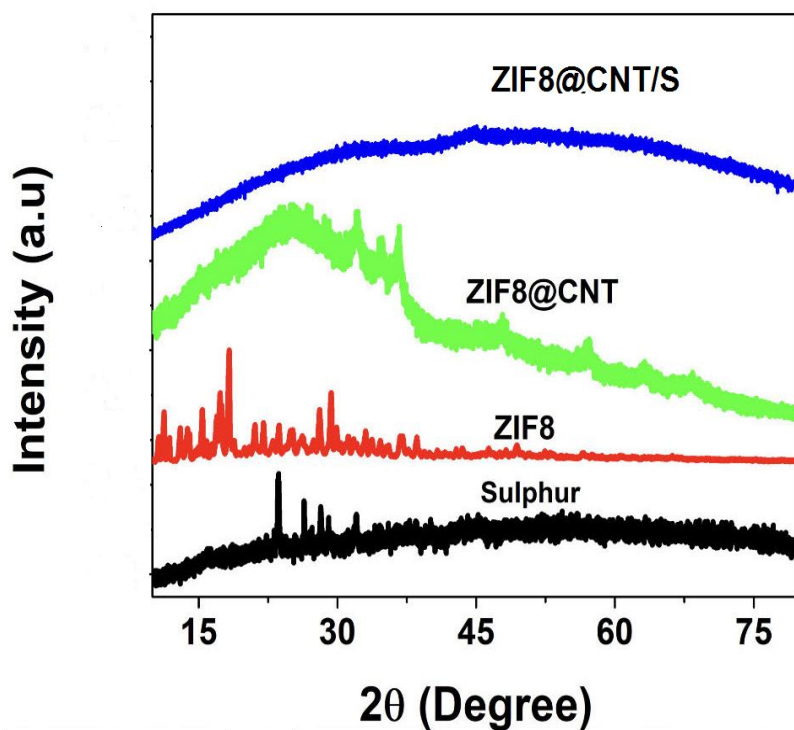


Fig.3.2 pXRD images of (a) Sulfur (b)Zeolite imidazole framework/8 (c)ZIF/8-Carbon-nanotubes (d) ZIF/8-Carbon-nantotubes/sulfur

3.1.2 Scanning Electron Microscope

SEM images have shown the presence of rhombohedral dodecahedron shaped nanoparticles for ZIF/67 with diameter around 250 nanometres. ZIF/8 nanocrystals also show a rhombic dodecahedron shape with a mixture of {100} and {110} facets. ZIF/8 has a diameter around 50-140 nanometres. In the presence of CNTs the diameter is much more uniform as the MOFs are attached to it. The pores on the ZIF-Carbon-nanotubes are also clearly visible.

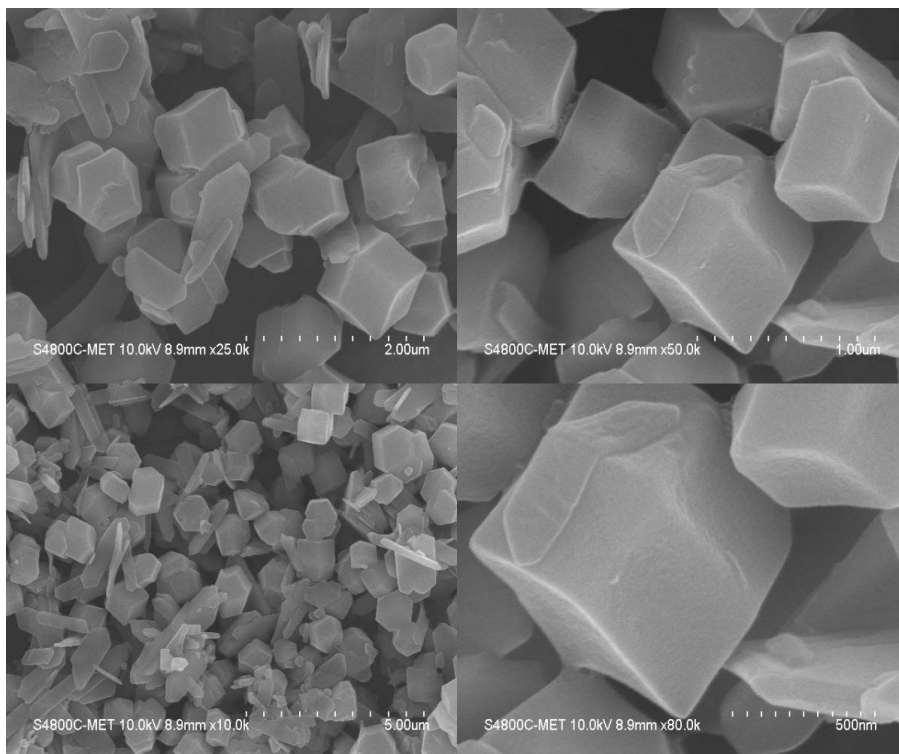


Fig.3.3 Electron Microscope images of ZIF/8

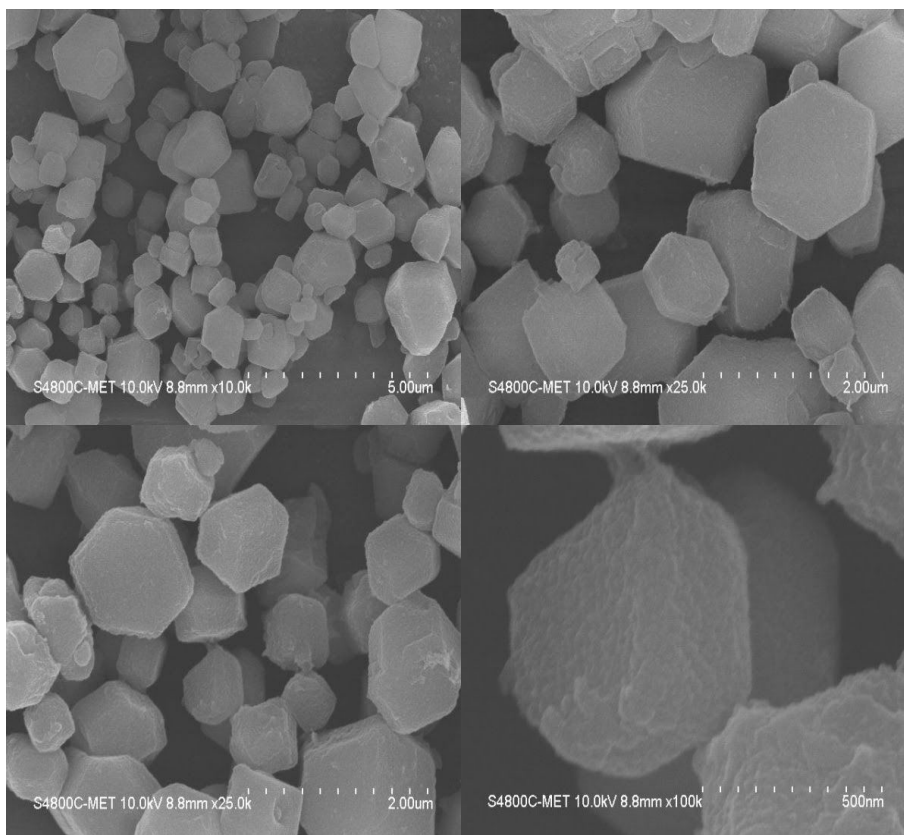


Fig.3.4 Electron Microscope images of ZIF/67.

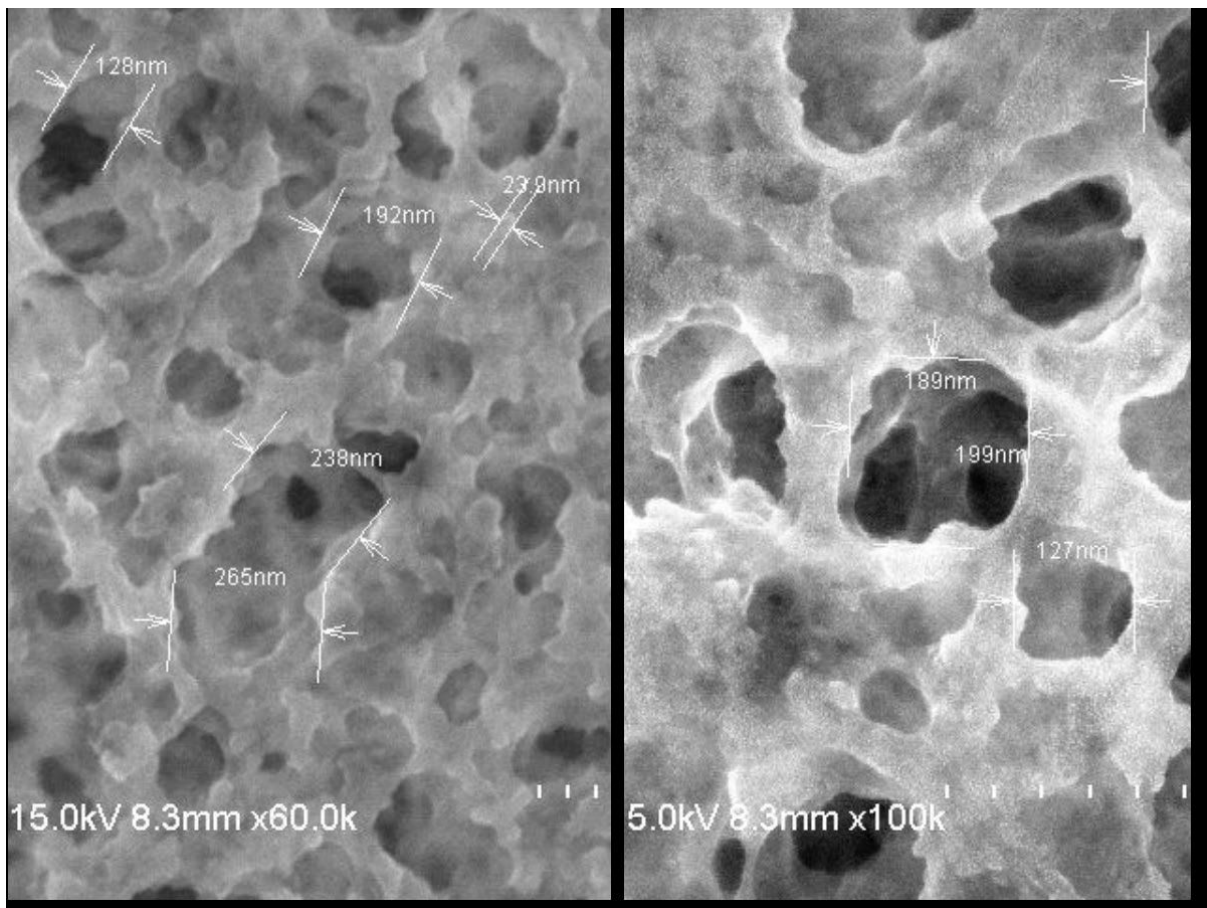


Fig.3.5 (a)SEM images of ZIF/67-Carbon Nanotubes showing pores.(b)SEM images of ZIF/8-carbon nanotubes

3.2 Flaws in Slurry preparation

3.2.1 Different slurry preparation

During the coating of the cathode on aluminum sheet ,the slurry prepared from 75%of the obtained composites ,15% conducting carbon and 10% poly vinylidene fluoride in nmp did not give an homogenous mixture.Multiple trials with different weight ratios of composites were carried out ,still leading to the same issues.The slurry was also scaled up to higher amounts from 100mg to 2g ,but the coating still appeared non-homogenous.



Fig.3.6 Non homogeneous slurry after coating on the sheets.

3.2.2 Discussion on why it might have happened

The reason for this to happen could not be understood properly. This can be due to moisture that the sulfur infused active particles are separating out of the PVDF-nmp solution as the active mixture is moisture sensitive. To avoid this, the slurry was heated at a low temperature for 1 hour under stirring. This did not solve the ongoing issue. As Pune has an average moisture content of 59.3% in the atmosphere, the slurry always tended to absorb the moisture. A sulfur coin cell was made with 50% conducting carbon, 40% sulfur, and ten %pvdf in nmp, which had a better coating. An open cell voltage of around 3.3V was obtained, which had a weight of around 0.89g. But again, the capacity was found to be really low around 700 mAhg⁻¹(from theoretical value), which then rapidly dropped to zero. This also can be explained due to the lack of homogeneity in the slurry mixture. After multiple attempts to fix the slurry preparation, it never succeeded. This way of slurry preparation was reported in multiple reports for ZIF/67-CNTs but couldn't be reproduced under the conditions worked on. Thus after multiple trials and due to lack of success, this

project then used the same ZIF/8 and ZIF/67 in PVP to produce separators for electrochemical processes.

3.3 Electrospinning analysis

The electrospinning technique of both ZIF/8 and ZIF/67 was done and successfully obtained. The voltage needed was around 12 kilo volt, with a flowrate of 0.5 ml/hr and drum speed of 1013 rpm. This was run for a total of 10 mL homogeneous solution of polymer and MOF and ran for 10-15 hours for each sample. The needle was kept 6.5 cm away from the collector (standardized).

3.3.1 Scanning electron microscope

The diameter from SEM images was found to be around 150 - 300 nm. The polymer concentration could be varied to change the diameter of the obtained fibres. This SEM images shows homogeneity of the ZIF/8 in the electrospun fibres.

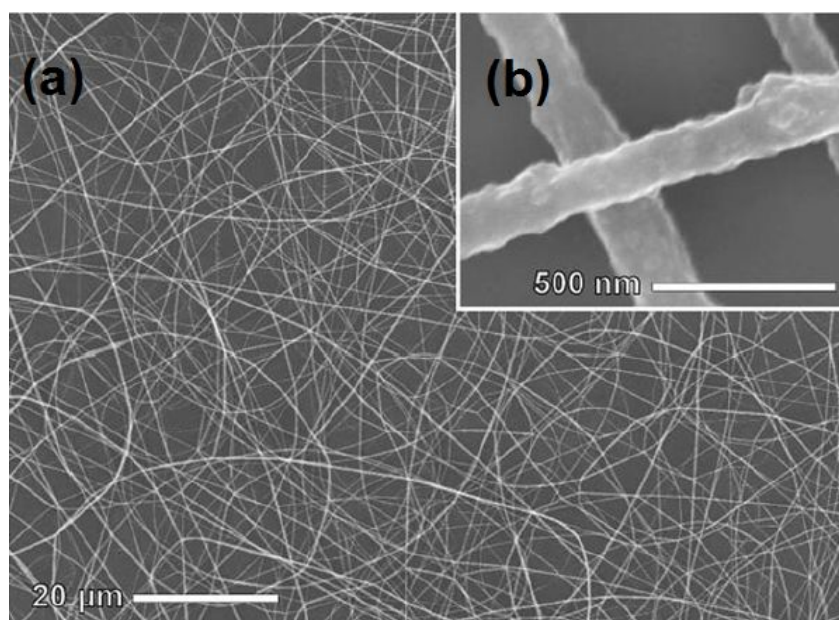


Fig.3.7 (a) ZIF/8 in polyvinylpyrrolidone at lower resolution

(b) ZIF/8 in polyvinylpyrrolidone at higher resolution

3.3.2 TEM images

TEM shows a homogeneous distribution of the Zeolitic imidazole framework on the polymeric surface within the fibres.

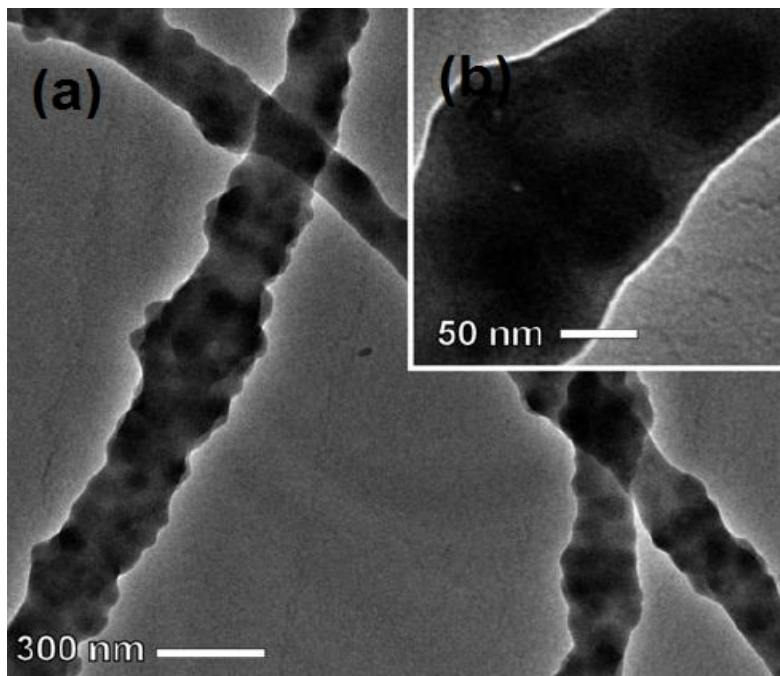


Fig.3.8 (a) TEM images of ZIF/8 in polyvinylpyrrolidone at lower resolution
(b)TEM images of ZIF/8 in polyvinylpyrrolidone at higher resolution

3.3.3 Images of the fibers obtained.

The digital images of the ZIF/8 in polyvinylpyrrolidone and ZIF/67 in polyvinylpyrrolidone are shown below. These images show homogeneous distribution across the aluminum foil.



Fig.3.9 (a) ZIF/8 in poly vinyl pyrrolidone

(b) ZIF/67 in poly vinyl pyrrolidone

3.3.4 Discussion on how the fibres will be used.

This obtained electrospun fibres could be used in multiple ways for the electrochemical processes. The preparation of this nanofiber with high porosity, large surface area has been a challenge and MOFs are well known for highly porous morphology and effective surface region. The uses of the electrospun MOF fibres has not been reported, thus more work is being carried out in CMET on the electrochemical perspective of this ZIF/67 or ZIF/8 nanoparticles in poly vinyl pyrrolidone

4. Conclusion

In this report, cobalt-based ZIF/67 and zinc-based ZIF/8 were synthesized using SEM and PXRD, respectively. After the synthesis, both ZIF/67 and ZIF/8 underwent pyrolysis with similar conditions producing ZIF/67 carbon-nanotubes and ZIF/8 Carbon-nanotubes, respectively. Both the nanoparticles were then treated with sulfur using the impregnation method, thus obtaining ZIF/67-carbon-nanotubes/Sulfur and ZIF/8-Carbon-nanotubes/Sulfur, which is then characterized using pXRD data. But the progress in this work can shorten due to the issues faced during the coating of the cathode material. The slurry was absorbing a lot of moisture, which might be one of the reasons for the same. Thus proving, a different protocol might be taken to complete the process.

The electrospinning technique was then used to make use of the ZIF/8 and ZIF/67. A mixture of ZIF/67 in PVP produced a homogeneous mixture which was successful in making the nanofibers. Similarly, in the case of ZIF/8 producing homogeneous fibers. This was confirmed by SEM and TEM images. Thus this report succeeded in creating nanoparticles of MOFs using the electrospinning technique as not been reported elsewhere. This also has high surface areas and good accessibility. This MOF nanofibres can be used not just in electrochemical processes but also for gas separation and absorption.

5. Future Outlook

The future works regarding the electrospun MOF nanofibers are exciting. This could be highly efficient electrocatalysts as well as advanced electrodes in lithium batteries, supercapacitors, and water splitters. MOFs, as a whole, have been used for numerous applications. These electrospun fibres can undergo pyrolysis and be used as slurry material for Lithium-ion batteries.

Although this report failed to produce positive results for MOFs in LSBs, the potential of the work is high. The advantages of using LSBs include high theoretical capacity around 1680 mAhg⁻¹ and gravimetric energy density of 2600 Watt hour per kilogram. This energy density is the combined use of sulfur-made electrode (1680 mAhg⁻¹) and lithiated electrode (3860 mAhg⁻¹). The noticeable advantage of MOFs include their ability to provide porous structures with uniformly manageable pore size and the ability to make use of their structure according to our needs. Done with the right protocol can achieve this potential.

The aim of this project was to create a better power source and, thus a better, eco-friendly, and effective energy for all human beings.

6. References

- [1] R. Demir-Cakan, M. Morcrette, F. Nouar, C. Davoisne, T. Devic, D. Gonbeau, R. Dominko, C. Serre, G. Ferey, J. M. Tarascon, *J. Am. Chem. Soc.* **2011**, 133, 16154.
- [2] Y. Huang, M. Zheng, Z. Lin, B. Zhao, S. Zhang, J. Yang, C. Zhu, H. Zhang, D. Sun, Y. Shi, J. Mater. Chem. A **2015**, 3, 10910.
- [3] Y. Son, J. S. Lee, Y. Son, J. H. Jang, J. Cho, *Adv. Energy Mater.* **2015**, 5, 1500110
- [4] Y. S. Su, A. Manthiram, *Nat. Commun.* **2012**, 3, 1166.
- [5] R. Fang, S. Zhao, Z. Sun, D. W. Wang, H. M. Cheng, F. Li, *Adv. Mater.* **2017**, 1606823
- [6] A.J. Howarth, Y.Y. Liu, P. Li, Z.Y. Li, T.C. Wang, J.T. Hupp, O.K. Farha, *Nat. Rev. Mater.* **2016** 1,15018.
- [7] M.W. Erba, D. Banerjee, S. Ghose, B.K. Medasani, A.K. Shukla, B.A. Legg, Y. Zhou, Z. Zhu, M.L. Sushko, J.J. De Yoreo, J. Liu, P.K. Thallapally, S.L. Billinge, *Nanoscale* **2018**, 10, 4291–4300
- [8] G. Zheng, Y. Yang, J. J. Cha, S. S. Hong, Y. Cui, *Nano Lett.* **2011**, 11, 4462
- [9] T. Nagaura, K. Tozawa, *Prog. Batteries Sol. Cells* **1990**, 9, 209.
- [10] Q. Zhang, Y. Wang, Z. W. Seh, Z. Fu, R. Zhang, Y. Cui, *Nano Lett.* **2015**, 15, 3780.
- [11] C. Wang, X. Wang, Y. Yang, A. Kushima, J. Chen, Y. Huang, J. Li, *Nano Lett.* **2015**, 15, 1796.
- [12] R. Fang, S. Zhao, Z. Sun, D. W. Wang, H. M. Cheng, F. Li, *Adv. Mater.* **2017**, 1606823
- [13] X. Fang, H. Peng, *Small* **2015**, 11, 1488.
- [14] X. Li, J. Liang, K. Zhang, Z. Hou, W. Zhang, Y. Zhu, Y. Qian, *Energy Environ. Sci.* **2015**, 8, 3181.
- [15] C. A. Milroy, S. Jang, T. Fujimori, A. Dodabalapur, A. Manthiram, *Small* **2017**, 13, 1603786.
- [16] S. Rehman, K. Khan, Y. Zhao, Y. Hou, *J. Mater. Chem. A* **2017**, 5, 3014.
- [17] M. Wild, L. O'Neill, T. Zhang, R. Purkayastha, G. Minton, M. Marinescu, G. J. Offer, *Energy Environ. Sci.* **2015**, 8, 3477.
- [18] S.-H. Chung, A. Manthiram, *Electrochim. Acta* **2013**, 107, 569.
- [19] S. H. Chung, A. Manthiram, *Adv. Mater.* **2014**, 26, 1360.
- [20] Z. Zhang, L.-L. Kong, S. Liu, G.-R. Li, X.-P. Gao, *Adv. Energy Mater.* **2017**, 7, 1602543
- [21] B.-C. Yu, J.-W. Jung, K. Park, J. B. Goodenough, *Energy Environ. Sci.* **2017**, 10, 86.
- [22] F. Zeng, K. Yuan, A. Wang, W. Wang, Z. Jin, Y.-S. Yang, *J. Mater. Chem. A* **2017**, 5, 5559.
- [23] Z. Peng, W. Fang, H. Zhao, J. Fang, H. Cheng, T.N.L. Doan, J. Xu, P. Chen, *J. Power Sources* 282 **2015** 70–78.
- [24] Y. Xu, Y. Wen, Y. Zhu, K. Gaskell, K.A. Cychosz, B. Eichhorn, K. Xu, C. Wang, *Adv. Funct. Mater.* 25 **2015** 4312–4320.

- [25] A. Rosenman, E. Markevich, G. Salitra, Y. Talyosef, F. Chesneau, D. Aurbach, J. Electrochem. Soc. 163 **2016** A1829–A1835.
- [26] R. Elazari, G. Salitra, A. Garsuch, A. Panchenko, D. Aurbach, Adv. Mater. 23 **2011** 5641–5644.
- [27] J.G. Wang, K. Xie, B. Wei, Nano Energy 15 **2015** 413–444.
- [28] M. Yu, R. Li, M. Wu, G. Shi, Energy Storage Mater. 1 **2015** 51–73.
- [29] K. J. Lee, J. H. Lee, S. Jeoung and H. R. Moon, Acc. Chem. Res., **2017**, 50, 2684–2692.
- [30] M. Zhao, Q. Lu, Q. Ma and H. Zhang, Small Methods, **2017**, 1, 16000310.
- [31] L. Chen, R. Luque and Y. Li, Chem. Soc. Rev., **2017**, 46, 4614–4630.
- [32] B.Y. Xia, Y. Yan, N. Li, H.B. Wu, X.W. Lou, X. Wang, Nat. Energy 1 **2016** 15006.
- [33] G. Ferey, Chem. Soc. Rev., **2008**, 37, 191–214.
- [34] Huali Wua, Yao Lia, Juan Rena, Dewei Raob, Qiaoji Zhenga, Liang Zhouc,*, Dunmin Lina Nano Energy 55 **2019** 82–92
- [35] Peng Chee Tan,* Boon Seng Ooi, Abdul Latif Ahmad and Siew Chun Low **2017** 1 215–226
- [36] J. Chen, D. Wu, E.D. Walter, M.H. Engelhard, P. Bhattacharya, H. Pan, Y. Shao, F. Gao, J. Xiao, J. Liu, Nano Energy 13 **2015** 267–274.